Supplementary methods

I. General and Surgical Procedures

Three male rhesus monkeys (*Macaca mulatta*, 9 and 10 kg) were used in these experiments. All experimental procedures were in accordance with National Institutes of Health Guide for the Care and Use of Laboratory Animals, the Society for Neuroscience Guidelines and Policies, and Stanford University Animal Care and Use Committee. General surgical procedures have been described previously[1]. Each animal was surgically implanted with a titanium head post, two recording chambers and a scleral eye coil. Surgery was conducted using aseptic techniques under general anesthesia (isoflurane) and analgesics were provided during postsurgical recovery. Structural magnetic resonance imaging was performed to locate the arcuate sulcus and prelunate gyrus in one of the monkeys for the placement of a recording chamber in a subsequent surgery. A craniotomy was performed in the two recording chambers on each animal, allowing access to the FEF and area V4.

II. Behavioral tasks

Measurement of target selection. The FEF has a well-established role in the control of visually guided saccadic eye movements[2]. Recently, it has become evident that this area is also involved in covert spatial attention[3,4]; i.e. attention to visual targets even when saccades are not initiated. This evidence demonstrates that the mechanisms controlling saccadic preparation and the deployment of visual spatial attention are highly overlapping, and perhaps complimentary[5]. Thus, in addition to studying the effects of our pharmacological manipulation of FEF activity on the neural signatures of attention within visual cortex, we also sought to assess its effects on saccadic target selection in the same

experiments. To measure target selection, we quantified a monkey's tendency to select stimuli at a particular location as the target of a saccadic eye movement, we employed a free-choice, saccade task similar to ones used previously in several studies[6,7] (Supplementary Fig. 1). In the task, the monkey was rewarded for making saccades to any one of two visual stimuli (0.5° diameter) appearing at diametrically opposed locations. One of the stimuli was positioned at the center of the FEF_{RF}. The appearance of the two stimuli on a given trial occurred within a range of temporal onset asynchronies (TOAs), from trials in which the FEF_{RF} appeared first (positive TOAs) to trials in which the FEF_{RF} appeared second (negative TOAs). The range of TOAs for a given block of trials was typically -80 to 320 ms, with 10 discrete TOA conditions evenly spaced within that range, excluding zero. Trials were randomly interleaved such that on any given trial the monkey could not predict the TOA. In a given experiment, at least 2 blocks of free-choice saccade trials were collected, one prior to FEF infusion and one following it. Each block consisted of at least 10 trials/TOA.

Each pair of pre and post-infusion free-choice saccade blocks could be used to compare the probability that the monkey would choose one target over the other as a function of TOA. For each of the two, we fit the data with a logistic regression function:

$$1/(1+\exp(a * (b-TOA)))$$

where b is the TOA at which the proportion of saccade choices is equal. This allowed us to measure the TOA at which the monkey was equally likely to choose either target. We refer to the point of equal choice probability (b) as the "point of equal selection" (PES). Similar to the studies cited above, the PES for a given block of trials was seldom zero, indicating that the monkey typically had a default preference for one of the target

locations. In addition, as has been observed in drug infusion studies[7] and electrical microstimulation studies[8] involving saccade-related areas, we observed that monkeys showed a general tendency to choose non-FEF_{RF} targets over FEF_{RF} targets. As a result, the overall mean PES was greater than 0 (mean = 58.05 ± 11.17; $p < 10^{-3}$). We interpret the overall bias toward non-FEF_{RF} targets as either the result of the presumed deleterious effects of repeated volume injections made into a restricted region of cortex or behavioral compensation for microstimulation-evoked saccades into the FEF_{RF}, or both. Regardless of the basis for this bias, and in spite of it, as in previous studies, we could nonetheless measure the behavioral effect of an infusion into the FEF as the *change* in PES from control values measured in the same experimental session.

Measurement of V4 responses during fixation. Responses of single V4 neurons to RF stimuli were measured during periods of passive fixation in a delayed saccade task[9]. In this task, a visual stimulus was presented within the RF of a V4 neuron 200 ms after the monkey fixated the fixation spot. The RF stimulus then remained on the display throughout the trial. Following 1 second of fixation and RF stimulation, the fixation spot was removed and one of two events occurred. On half of the trials, the fixation spot reappeared at one of two locations within the hemifield opposite the RF and the monkey was rewarded for shifting its gaze to that point. On the remaining half of trials, the fixation spot did not reappear and the monkey was instead rewarded for shifting its gaze to the RF stimulus. The two saccade conditions were randomly interleaved such that the monkey could not predict where the saccade would subsequently be made until the fixation spot was removed. In some experiments, a stimulus was flashed briefly (13 ms) at a random time and location distant from the V4 RF as a potential distracter. However,

we observed no consistent effect of the flashed stimulus on V4 responses, and thus, data from experiments with and without the flashed stimulus were combined. All of the analyses of V4 responses were performed on the period of the trial prior to fixation spot offset and during stable fixation.

Eye position measurement. Eye position was monitored with a scleral search coil and digitized at 500 Hz (CNC Engineering, Seattle, WA). The spatial resolution of eye position measurements was <<0.1° in both monkeys and our system allowed us to easily detect displacements of that size on individual trials.

Visual Stimuli. All stimuli were presented on a 29° x 39° colorimetrically calibrated CRT monitor (Mitsubishi Diamond Pro 2070SB-BK) with medium short persistence phosphors. Visual stimuli presented to V4 RFs were 1.2 – 1.9° x 0.2 – 0.4° bar stimuli appearing at 4 possible orientations (0, 45, 90 and 135° θ). Stimulus presentation, data acquisition and behavioral monitoring were controlled by CORTEX system.

III. Electrophysiology

Single-neuron recordings. Recordings of single neurons in area V4 were made through a surgically implanted cylindrical titanium chamber (20 mm diameter) overlaying the prelunate gyrus. Electrodes were lowered into the cortex using a hydraulic microdrive (Narashige, Tokyo, Japan). Activity was recorded extracellularly with varnish-coated tungsten microelectrodes (FHC Inc., Bowdoinham, ME) of 0.2–1.0 MΩ impedance (measured at 1 KHz). Extracellular waveforms were digitized and classified as single neurons using online template-matching and window-discrimination techniques (FHC Inc., Bowdoinham, ME).

Localization and electrical microstimulation of the FEF. During each experiment, a site within the FEF was first localized by our ability to evoke fixed-vector, saccadic eye movements with stimulation at currents of ≤50 μA[10]. Electrical microstimulation consisted of a 100 ms train of biphasic current pulses (0.25 ms, 200 Hz) delivered with a Grass stimulator (S88) and two Grass stimulation isolation units (PSIU-6) (Grass Instruments, West Warwick, RI). Current amplitude was measured via the voltage drop across a 1 kΩ resistor in series with the return lead of the current source. During each experimental session, we mapped the saccade vector elicited via microstimulation at the cortical site under study with the use of a separate behavioral paradigm[3]. In this paradigm, the monkey was required to fixate on a visual stimulus (0.5° diameter circle) for 500 ms, after which a 100-ms stimulation train was delivered on half the trials. The endpoint of the evoked saccade vector was used to define the "response field" of the FEF site (FEF_{RF}).

IV. Local infusion of drugs into the FEF

Using a custom-designed system[11], we infused 0.5 – 1.0 μL of drug into intracortical sites within the FEF. Our system consisted of a 32-gauge (236 μm outer diameter) stainless steel cannula containing a 75 μm, commercially available epoxy-coated, tungsten microelectrode (FHC Inc., Bowdoinham, ME). The microelectrode was held in place inside the cannula via a cilux T-junction. The electrode was passed through the center of the T-junction and through a plastic ferrule where it was soldered to a connector for recording. The cannula was attached to a different opening of the T-junction via another ferrule. To the last of the T-junction openings was attached the drug

line which consisted of a third ferrule that attached 363 μm (outer diameter) polyimide-coated glass tubing (Polymicro Technologies, Phoenix, AZ) to the junction. The polyimide tubing was then connected to a manual injection drive (Stoelting, Wood Dale, IL) and a gas-tight microsyringe (Hamilton, Reno, NV) via a series of high precision fluidic valves attached to a fluidic 'circuit' board. The T-junctions, ferrules, fluid valves and fluidic circuit board were all obtained from LabSmith (Livermore, CA). Since the inner diameters of the tubing and the cannula were equal (150 μm), drug flow was steady with a minimum of clogging or hysteresis.

To measure fluid flow into the brain, we drew up into the fluid path an oil-dye-oil marker, that could be observed with the naked eye, moving inside of the polyimide tubing. The oil in the marker was of low viscosity (~1 *centistokes*) and the dye was food coloring. Within the 150-μm tubing, a 1 cm movement of the marker equaled a ~170 nL movement of the drug out of the cannula. Since we could measure at least 1 mm movements with the naked eye, the volume resolution of the infusion system was <17 nL. The inclusion of the tungsten microelectrode within the center of the drug cannula further allowed us to record the activity of single neurons near the center of the delivered drug volume within conventional recording and filtering. Moreover, we could also use standard electrical microstimulation to confirm at each drug site that saccades could be elicited with low currents, and to thus confirm that each infusion site was within the FEF. The microelectrode typically extended beyond the beveled tip of the cannula by 50 – 500 μm. To keep the microelectrode from being damaged when inserting the cannula into the brain, the ferrule connecting it to the T-junction could be rotating 3-turns counter-clockwise, thereby retracting the microelectrode about 1 mm back into the cannula. Once

the cannula was well within the brain, the ferrule could be slowly rotated clockwise and tightened thus positioning the electrode beyond the cannula opening at a known distance.

Infusion of SCH23390, quinpirole, muscimol and saline. Infusion of either SCH23390, quinpirole, muscimol (Sigma-Aldrich, St. Louis, MO) or physiological saline were made into the FEF of behaving monkeys using the above system. To manipulate D1R-mediated activity, we used SCH23390, a potent and selective D1-like receptor antagonist[12] that has been widely used to block D1Rs in both *in vitro*[13] and *in vivo* studies[14,15]. For SCH23390, we used a concentration of 5 mg/ml, which corresponds to the concentrations previously found to produce changes in the delay activity[16] and spatial tuning of dorsolateral PFC neurons in behaving monkeys[17] and change in reliability of synaptic transmission between pairs of frontal pyramidal neurons in vitro[18]. SCH23390 was prepared in sterile physiological saline and buffered with NaOH to a pH of 5.5 - 6 prior to each experiment. To inactivate FEF neuronal activity, we used muscimol, a potent and selective $GABA_a$ agonist that has been widely used in studies involving in vivo inactivation of local neuronal activity, particularly in behaving monkey studies[7,19,20]. As with SCH23390, and similar to previous studies, muscimol was dissolved in physiological saline at a concentration of 5 mg/ml (pH= 6.5-7). We used quinpirole, a selective D2 receptor agonist, to manipulate D2R-mediated activity within the PFC. Previous studies have shown that microiontophoretic application of this drug does not increase persistent activity, but rather increases the more saccade-related activity within the PFC[21]. Quinpirole was dissolved in physiological saline at 5 mg/ml concentration (pH=6.5 -7). Prior to delivery of any drug, the entire fluid delivery system was soaked and thoroughly flushed with cold sterilant (chlorhexidine diacetate, Nolvasan), flushed

with sterile water and then allowed to dry. For all three drugs and saline, a volume of 0.5 – 1.0 uL was infused into the FEF. Previous studies indicate that at such volumes, cortical tissue up to 1 – 1.7 mm from the infusion site should be affected by the drug[22]. We therefore assume that all drug infusions directly affected activity within all cortical layers.

V. Statistics & analyses

All data analysis was performed in Matlab (The MathWorks, Inc., Natick, MA). Only completed trials were included in the analysis.

Firing rate analyses. The responses of each V4 neuron to RF stimuli were converted to normalized values for analyses. Specifically, each neuron's response to each stimulus was divided by mean response of that neuron to both preferred and non-preferred stimuli before and after drug infusion. Changes in visual responses of V4 neurons were computed both as differences in normalized responses (i.e. $\Delta response = response_a - response_b$) and as modulation indices ($[response_a - response_b] / [response_a + response_b]$) to facilitate comparisons with other studies.

Receiver-operating characteristic (ROC) analysis. An ROC analysis was carried out on the distributions of firing rates of V4 neurons during the RF presentation of the most effective oriented bar stimulus and an orthogonal bar during a given block of trials. The areas under ROC curves were used as indices of stimulus selectivity and were calculated as in previous studies[23]. Specifically, we computed the average firing rate in a 100 ms window, moving from RF stimulus onset to the end of the trial at 20 ms steps. We then computed the probability that the firing rate in the 100 ms window for each stimulus condition exceeded a criterion. The criterion was incremented from 0 to the maximum

firing rate, and the probability of exceeding each criterion was computed. Thus, a single point on the ROC curve is produced for each increment in the criterion, and the entire ROC curve is generated from all of the criteria. The area under the ROC curve is a normalized measure of the separation between two firing rate distributions obtained with two RF stimuli, and provides an estimate of how well an ideal observer would be able to discriminate the two stimuli based solely on the firing rate distributions[23]. Differences in ROC areas, at the population level, were assessed by way of nonparametric tests on paired samples.

Reliability of V4 responses. As a measurement of the across-trial reliability of V4 neuronal responses we computed the Fano factor (FF). The FF was computed by calculating the variance divided by mean of the spike counts across trials in 100-ms windows centered on successive 20-ms time bins, for each set of identical trial conditions. Note that the FF measures across-trial variability [24] as opposed to within-trial variability of spike times or inter-spike intervals[25]. Windows with no spikes on any of the trials were excluded from FF calculations. To control for a possible effect of variable firing rates on FF, we used a method first introduced by Mitchell et al[26]. In this method mean and variance of firing rate were calculated for each 100 ms window of response of each cell. The window was moving by 20 ms steps. The calculated firing rates were then divided into 5 groups of <1, 1-2, 2-4, 4-8, > 8 spikes/ s. Supplementary Fig. 4 illustrates the line plot of average mean firing rate versus average firing rate variance for each group before and after SCH23390 infusion.

Detection of fixational eye movements/microsaccades. Microsaccade detection was performed as described elsewhere[27]. Microsaccades were defined as eye movements

which exceeded 0.1° amplitude and had maximum velocity greater than 10°/sec for at least 10ms. Additionally, points in 50ms windows prior to and following putative microsaccades were tested with a two sample Kolmogorov-Smirnov test ($p < 0.01$) to assess significant deflections relative to noise.

Statistical tests. A criterion level of $p < 0.05$ was used in all statistical analysis. P values $< 10^{-3}$ are reported as $p < 10^{-3}$. We used Wilcoxon signed-rank test to evaluate significance of differences between two paired populations or one population against zero. Other tests used throughout the text are mentioned in each instance.

Supplementary discussion

In addition to identifying dopamine D1Rs as mediating prefrontal control of visual cortical signals, the effects we observed during the D1R manipulation also provide a definitive demonstration that FEF neurons modulate activity within visual cortex. In a previous set of studies from this laboratory, electrical microstimulation was used to activate sites within the FEF that either overlapped retinotopically or did not overlap with the receptive fields (RFs) of area V4 neurons[28]. Those studies, and similar ones[e.g.29], provide strong evidence that the circuitry controlling top-down modulation of visual cortex involves the circuitry (including the FEF) known to control saccades. However, one important limitation of results from microstimulation studies is that one cannot infer a role of neurons at the stimulated site in causing the observed effects, if only because the possibility of antidromic activation of other brain structures cannot be ruled out[30]. More recently, additional caveats regarding the use of microstimulation have been introduced based on direct local[31] and system-wide[32] measurements of its effects. Thus, with respect to the role of the FEF in top-down control, the issue has gone unresolved. The present

results resolve this issue by showing that changes in FEF activity is sufficient to change visual responses in posterior visual cortex. In addition, the results demonstrate a role of dopamine D1Rs in the FEF's control of visual cortical signals.

The enhancement effects we observed in V4 (increased responses, selectivity, and reliability) were similar in magnitude to those observed with FEF microstimulation[28]. This fact suggests that the small fraction of FEF neurons expressing D1Rs (about 25%[33]) are a critical part of the circuitry that regulate interactions between the FEF and posterior visual areas. The effects of FEF inactivation with muscimol on V4 appeared less similar to the microstimulation results, which as one might have assumed, should simply have been the reverse of the enhancement effects. Instead, in the present results, we did not observe a decrement in the overall response magnitude. Importantly, in the original microstimulation study, the suppressive effects observed in V4, during microstimulation of *non-overlapping* FEF representations, were only about half the size of the enhancement effects[28]. The smaller suppressive effects may have been due to the relatively passive nature of the fixation task that did not require the monkey to attend to the RF stimulus. As a result, increasing the allocation of attention (e.g. via FEF microstimulation) may have been much easier than decreasing it. Moreover, suppression of V4 responses was only achieved when a competing, non-RF stimulus was also present in the visual display throughout the trial. The enhancement effects, though smaller without competing stimuli, were nonetheless still present. The current study did not include such a condition, which might explain the absence of a significant decrease in response magnitude. Nonetheless, the inactivation of the FEF with muscimol dramatically reduced the orientation selectivity of V4 neurons. This result is congruent

not only with the microstimulation results but also with those of a recent study showing that similar inactivation of the FEF reduces perceptual performance of monkeys discriminating the orientation of Landolt rings[34].

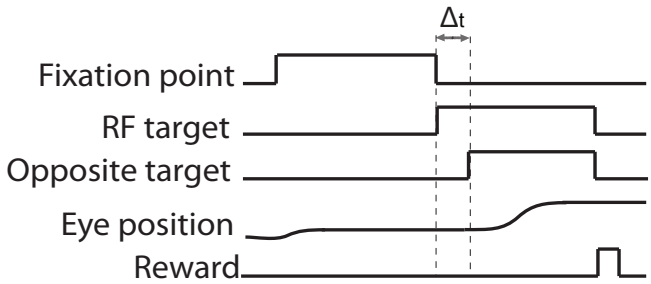

Supplementary Figure 1. Sequence of events in the free-choice saccade task. On each trial, the appearance of a visual stimulus is randomly varied such that either the FEF_{RF} target or a target in the opposite hemifield appears first. The temporal onset asynchrony is denoted by Δt. The monkey is rewarded for saccades made to either target.

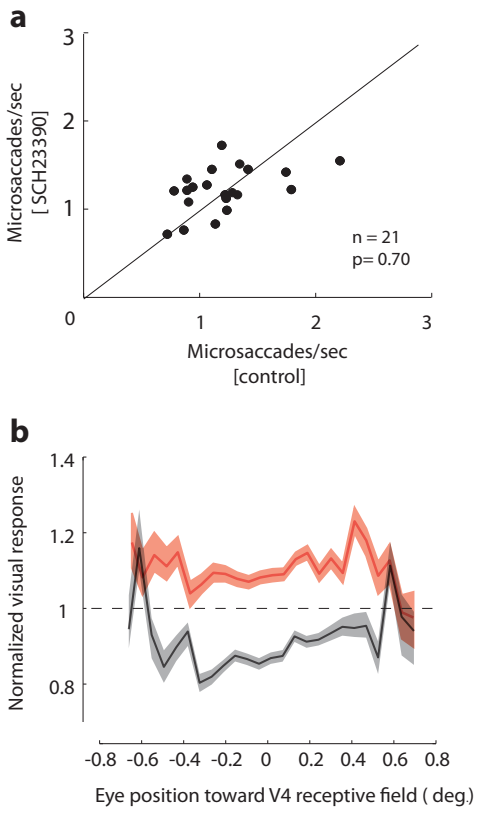

Supplementary Figure 2. a, Comparison of the rates of microsaccades during fixation before and after infusion of SCH23390 into FEF sites. Each point shows the mean microsaccade rate computed from all trials while a visual stimulus was presented within the $V4_{RF}$. All saccades with amplitudes >0.1° and <1° were counted as microsaccades. **b**, Normalized visual response of V4 neurons as a function of eye position before (gray) and after (red) the SCH23390 infusion into FEF sites. The mean response of all neurons with RFs that overlapped the FEF_{RF} is shown. Values on the ordinate denote bins of varying mean eye position, relative to the center of fixation spot and along an axis toward the $V4_{RF}$ center, computed from each trial. Both eye position and response values were measured within 100-ms time bins. A majority of eye positions (92% for both before and after infusion) were located within -0.5° and 0.5° of the center of the fixation spot.

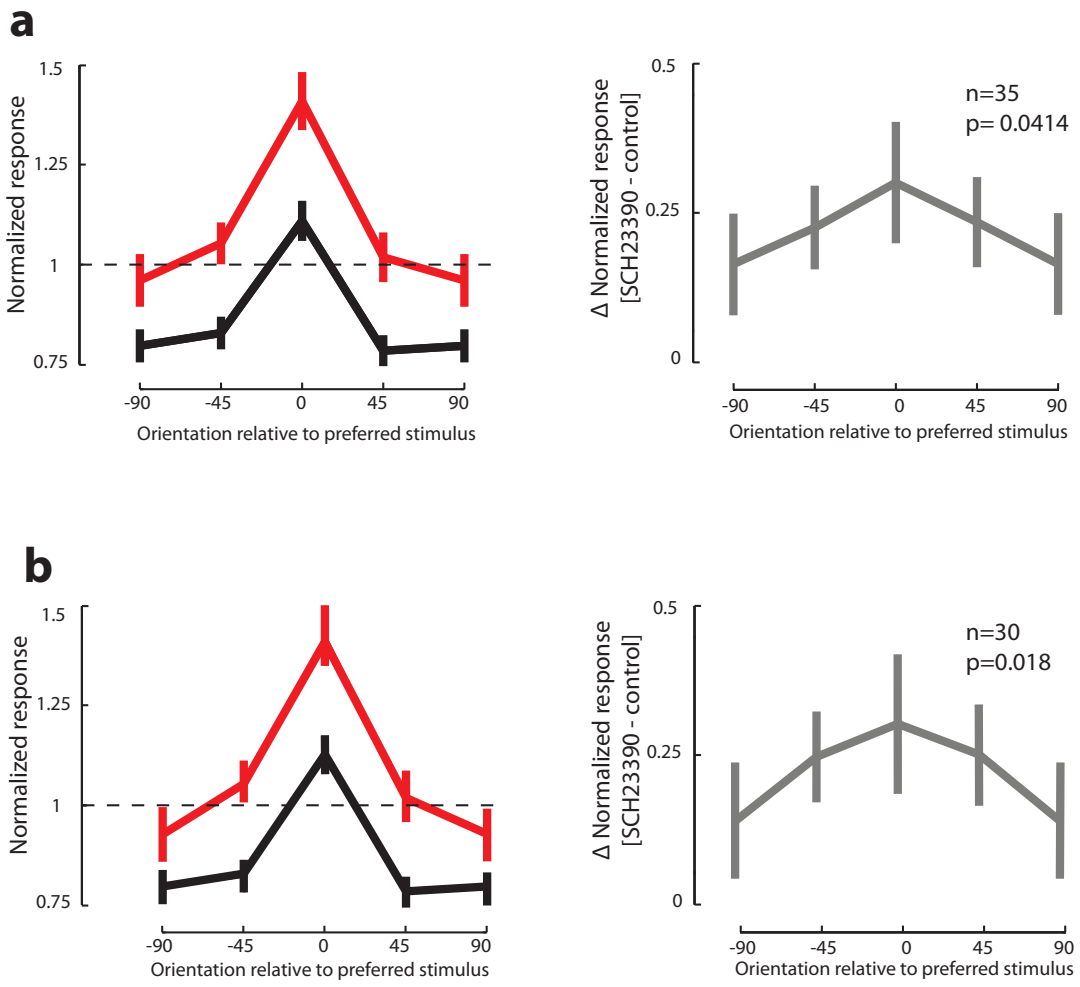

Supplementary Figure 3. Orientation tuning curves of V4 neurons before (black) and after (red) infusion of SCH23390 at overlapping FEF sites. **a**, Tuning curves for all 35 (of 37) neurons tested with 4 bar orientations. Left plot shows both control and post-SCH233390 curves and the right plot shows the difference function. Normalized response values denote the average response of each neuron normalized by its grand mean. **b**, Same as A, but data are from the subset of neurons with significant orientation tuning in the control measurement (n = 30). Note that the change in response following the SCH23390 infusion is greatest at the preferred orientation. P values shown denote the significance of the main effect of orientation (repeated-measures ANOVA).

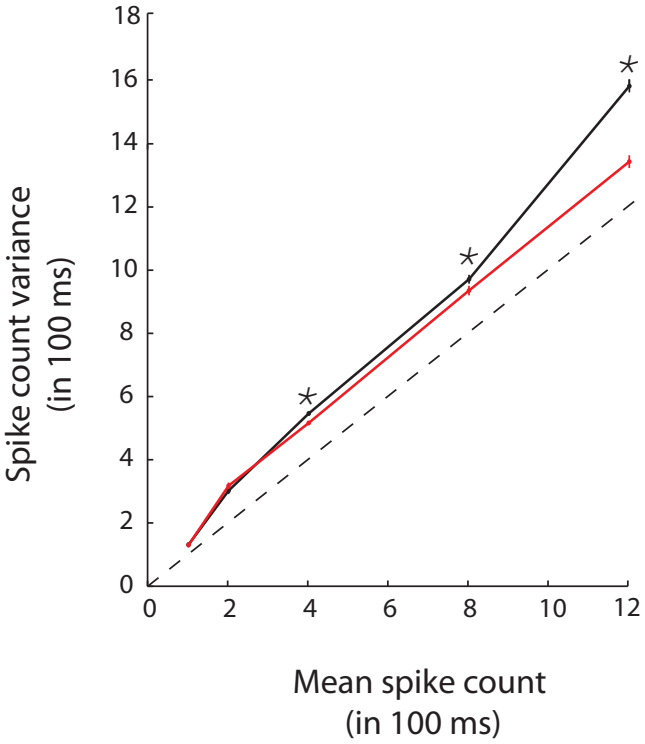

Supplementary Figure 4. Change in V4 response variance following SCH23390 is independent of mean spike count. Plot shows the relationship between mean spike count and spike count variance for V4 visual responses before (black) and after (red) the SCH23390 infusion into the FEF. The both values are from all neurons with RFs that overlapped the FEF_{RF}. Points on the two lines compare the variance at 5 equal mean spike counts. Asterisks denote significant differences between individual points (Mann-Whitney U test, $p < 0.001$). These data indicate that the reduction in Fano factor is not due to the increased firing rate observed after the SCH23390 infusion.

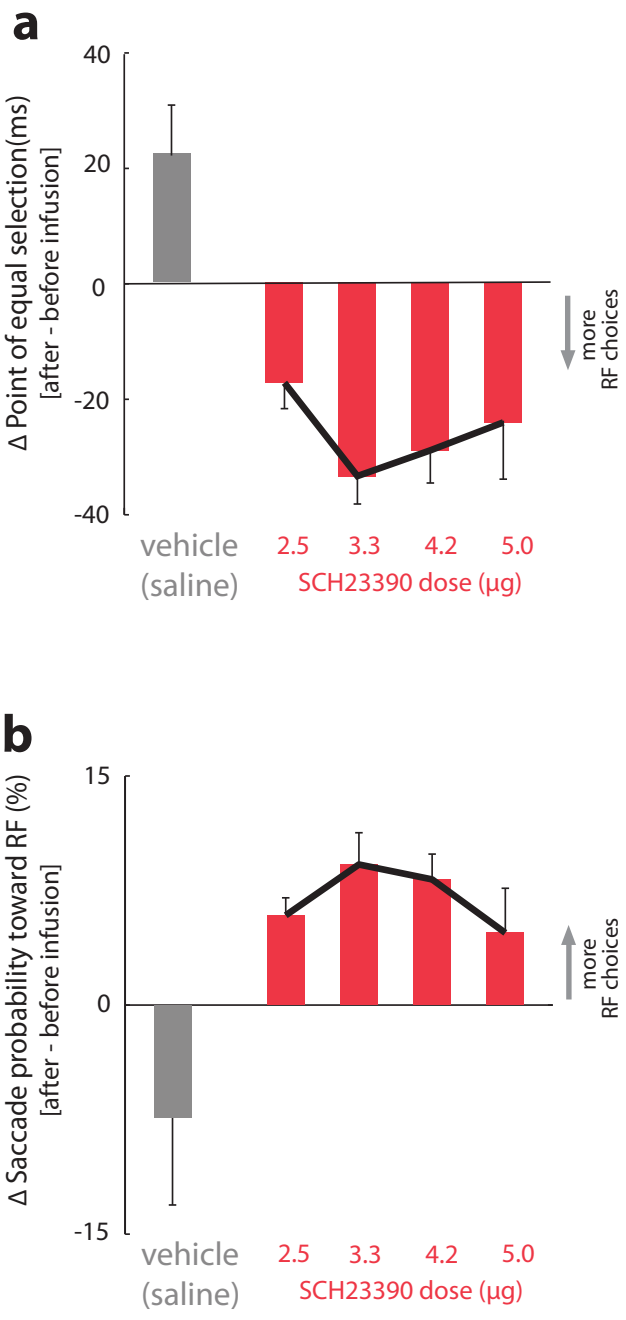

Supplementary Figure 5. Effect of the D1R manipulation on target selection across different dosages of SCH23390. **a**, The change in PES (reductions indicating increased likelihood of saccades to FEF_{RF} targets, arrow) following injections of the drug vehicle (saline) or across a range of SCH23390 dosages (2.5 – 5.0 µg). Selection of FEF_{RF} targets increased with SCH23390 compared to control (pre-injection) ($P < 0.001$), as well as compared to the effect of saline ($P<0.05$). **b**, Target selection data expressed in terms of overall saccade probability (positive values indicating increased likelihood of saccades to FEF_{RF} targets, arrow). For this measure, selection of FEF_{RF} targets also increased with SCH23390 compared to control (pre-injection) ($P < 0.05$), and compared to the effect of saline ($P<0.001$).

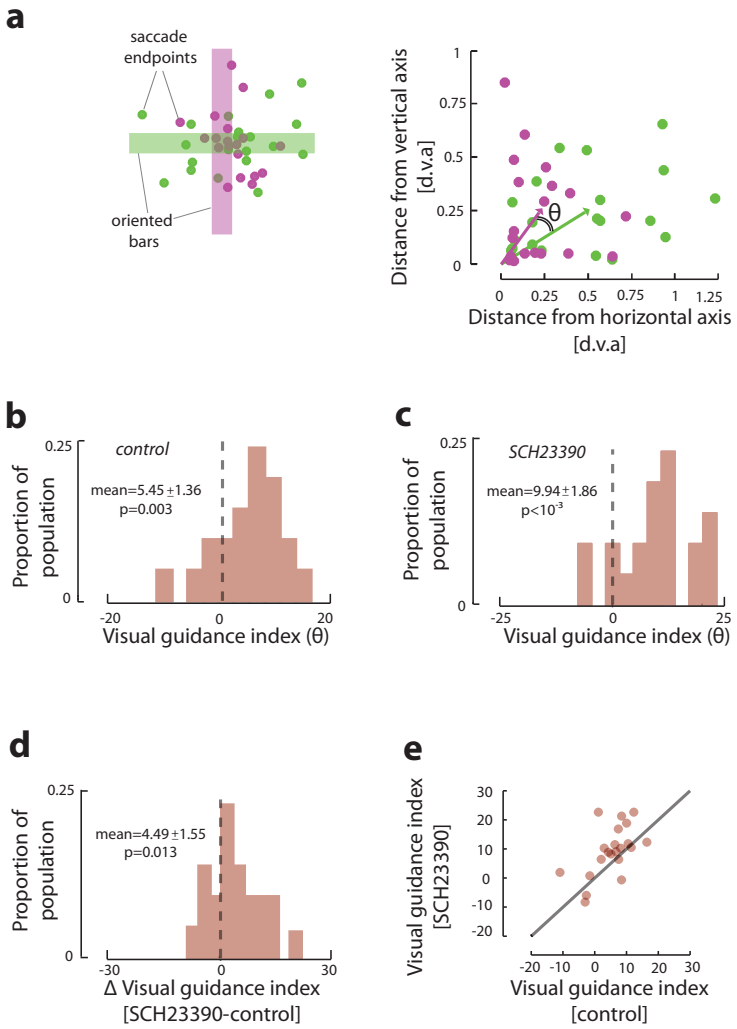

Supplementary Figure 6. Effects of the D1R manipulation on the orientation discriminability of visually guided saccades. The endpoints of saccades to the stimuli presented inside the RFs of V4 neurons were analyzed for evidence of an influence of orientation on saccade metrics, similar to Moore (1999)[35]. The distribution of distances of endpoints from the axis of stimulus orientation could be used to distinguish saccades to orientations differing by 90°. **a**, an example distribution of saccades to a vertical (purple) or horizontal(green) bar stimulus, and the corresponding distributions on endpoint distances from the two axes of orientation. The difference in the angle (θ) of the mean vectors of both distributions is taken as an index of orientation discriminability of the visually guided saccades. **b**, distribution of visual guidance indices during control trials

and (**c**) following the infusion of SCH23390 into the FEF site. **d**, distribution of changes in visual guidance following the SCH23390 infusion, and (**e**) a scatter plot comparing guidance indices before and after the drug manipulation. These data show an improvement in stimulus (orientation) discriminability of visually guided saccades following the D1R manipulation.

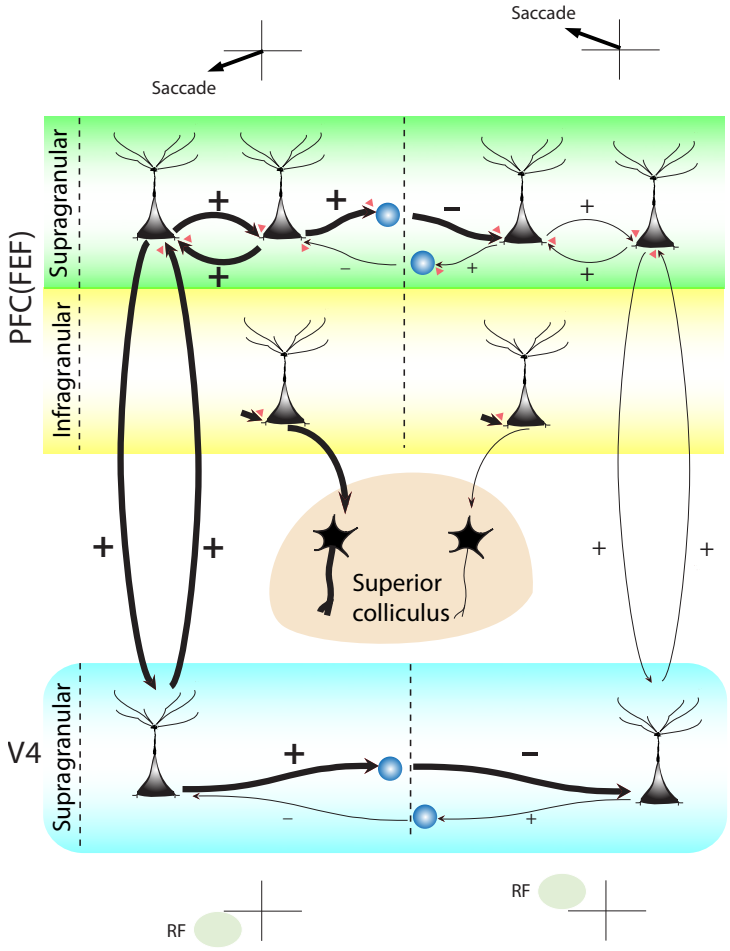

Supplementary Figure 7. Influence of D1Rs on recurrent networks within the PFC (specifically FEF) and between the PFC and V4. Recurrence within the PFC is thought to underlie the persistence of information (remembered saccades or locations). Recurrence between the PFC and V4 is proposed to determine the gain on visual inputs within V4. Intercolumnar inhibition via inhibitory interneurons (blue circles) contributes to competition between different saccadic and retinotopic representations (left and right columns) in the PFC and V4, respectively. Dopaminergic input from the ventral tegmental area to the PFC modulates (red triangles) both types of recurrence through D1Rs and influences the level of competition between spatial representations. For example, increases in recurrence in a particular column while remembering or attending to a corresponding location (thicker arrows at left) can be modulated by the level of dopamine. Biases in competition can also be achieved by experimental manipulation of

D1R-mediated activity, as in the present study. Also shown are the oculomotor projections from infragranular FEF neurons to the superior colliculus. Other anatomical details are omitted for simplicity.

References

1. Graziano,M.S., Hu,X.T. & Gross,C.G. Visuospatial properties of ventral premotor cortex. J. Neurophysiol. 77, 2268-2292 (1997).

2. Schall,J.D. & Hanes,D.P. Neural basis of saccade target selection in frontal eye field during visual search. Nature 366, 467-469 (1993).

3. Moore,T. & Fallah,M. Control of eye movements and spatial attention. Proc. Natl. Acad. Sci. U. S. A 98, 1273-1276 (2001).

4. Thompson,K.G., Biscoe,K.L. & Sato,T.R. Neuronal basis of covert spatial attention in the frontal eye field. J. Neurosci. 25, 9479-9487 (2005).

5. Moore,T., Armstrong,K.M. & Fallah,M. Visuomotor origins of covert spatial attention. Neuron 40, 671-683 (2003).

6. Schiller,P.H. & Tehovnik,E.J. Neural mechanisms underlying target selection with saccadic eye movements. Prog. Brain Res. 149, 157-171 (2005).

7. Wardak,C., Olivier,E. & Duhamel,J.R. Saccadic target selection deficits after lateral intraparietal area inactivation in monkeys. J. Neurosci. 22, 9877-9884 (2002).

8. Tehovnik,E.J., Slocum,W.M. & Schiller,P.H. Differential effects of laminar stimulation of V1 cortex on target selection by macaque monkeys. Eur. J. Neurosci. 16, 751-760 (2002).

9. Moore,T. & Chang,M.H. Presaccadic discrimination of receptive field stimuli by area V4 neurons. Vision Res. 49, 1227-1232 (2009).

10. Bruce,C.J., Goldberg,M.E., Bushnell,M.C. & Stanton,G.B. Primate frontal eye fields. II. Physiological and anatomical correlates of electrically evoked eye movements. J. Neurophysiol. 54, 714-734 (1985).

11. Noudoost,B. & Moore,T. A reliable microinjectrode system for use in behaving monkeys. J. Neurosci. Methods 194, 218-23 (2010).

12. Bourne,J.A. SCH 23390: the first selective dopamine D1-like receptor antagonist. CNS. Drug Rev. 7, 399-414 (2001).

13. Nicola,S.M., Kombian,S.B. & Malenka,R.C. Psychostimulants depress excitatory synaptic transmission in the nucleus accumbens via presynaptic D1-like dopamine receptors. J. Neurosci. 16, 1591-1604 (1996).

14. Lanteri,C. et al. Inhibition of monoamine oxidases desensitizes 5-HT1A autoreceptors and allows nicotine to induce a neurochemical and behavioral sensitization. J. Neurosci. 29, 987-997 (2009).

15. Rossato,J.I., Bevilaqua,L.R., Izquierdo,I., Medina,J.H. & Cammarota,M. Dopamine controls persistence of long-term memory storage. Science 325, 1017-1020 (2009).

16. Williams,G.V. & Goldman-Rakic,P.S. Modulation of memory fields by dopamine D1 receptors in prefrontal cortex. Nature 376, 572-575 (1995).

17. Vijayraghavan,S., Wang,M., Birnbaum,S.G., Williams,G.V. & Arnsten,A.F. Inverted-U dopamine D1 receptor actions on prefrontal neurons engaged in working memory. Nat. Neurosci. 10, 376-384 (2007).

18. Gao,W.J., Krimer,L.S. & Goldman-Rakic,P.S. Presynaptic regulation of recurrent excitation by D1 receptors in prefrontal circuits. Proc. Natl. Acad. Sci. U. S. A 98, 295-300 (2001).

19. Dias,E.C. & Segraves,M.A. Muscimol-induced inactivation of monkey frontal eye field: effects on visually and memory-guided saccades. J. Neurophysiol. 81, 2191-2214 (1999).

20. Sommer,M.A. & Tehovnik,E.J. Reversible inactivation of macaque frontal eye field. Exp. Brain Res. 116, 229-249 (1997).

21. Wang,M., Vijayraghavan,S. & Goldman-Rakic,P.S. Selective D2 receptor actions on the functional circuitry of working memory. Science 303, 853-856 (2004).

22. Martin,J.H. & Ghez,C. Impairments in reaching during reversible inactivation of the distal forelimb representation of the motor cortex in the cat. Neurosci. Lett. 133, 61-64 (1991).

23. Britten,K.H., Shadlen,M.N., Newsome,W.T. & Movshon,J.A. The analysis of visual motion: a comparison of neuronal and psychophysical performance. J. Neurosci. 12, 4745-4765 (1992).

24. Churchland,M.M., Yu,B.M., Ryu,S.I., Santhanam,G. & Shenoy,K.V. Neural variability in premotor cortex provides a signature of motor preparation. J. Neurosci. 26, 3697-3712 (2006).

25. de Ruyter van Steveninck RR, Lewen,G.D., Strong,S.P., Koberle,R. & Bialek,W. Reproducibility and variability in neural spike trains. Science 275, 1805-1808 (1997).

26. Mitchell,J.F., Sundberg,K.A. & Reynolds,J.H. Differential attention-dependent response modulation across cell classes in macaque visual area V4. Neuron 55, 131-141 (2007).

27. Armstrong,K.M., Fitzgerald,J.K. & Moore,T. Changes in visual receptive fields with microstimulation of frontal cortex. Neuron 50, 791-798 (2006).

28. Moore,T. & Armstrong,K.M. Selective gating of visual signals by microstimulation of frontal cortex. *Nature* **421**, 370-373 (2003).

29. Ekstrom,L.B., Roelfsema,P.R., Arsenault,J.T., Bonmassar,G. & Vanduffel,W. Bottom-up dependent gating of frontal signals in early visual cortex. Science 321, 414-417 (2008).

30. Tehovnik,E.J., Tolias,A.S., Sultan,F., Slocum,W.M. & Logothetis,N.K. Direct and indirect activation of cortical neurons by electrical microstimulation. *J. Neurophysiol.* **96**, 512-521 (2006).

31. Histed,M.H., Bonin,V. & Reid,R.C. Direct activation of sparse, distributed populations of cortical neurons by electrical microstimulation. *Neuron* **63**, 508-522 (2009).

32. Logothetis,N.K. *et al.* The effects of electrical microstimulation on cortical signal propagation. *Nat. Neurosci.* **13**, 1283-1291 (2010).

33. Santana,N., Mengod,G. & Artigas,F. Quantitative analysis of the expression of dopamine D1 and D2 receptors in pyramidal and GABAergic neurons of the rat prefrontal cortex. *Cereb. Cortex* **19**, 849-860 (2009).

34. Monosov,I.E. & Thompson,K.G. Frontal eye field activity enhances object identification during covert visual search. *J. Neurophysiol.* **102**, 3656-3672 (2009).

35. Moore,T. Shape representations and visual guidance of saccadic eye movements. Science 285, 1914-1917 (1999).